Netsu Sokutei **33** (4) 167-173

解　説

High-Resolution Thermal Expansion of Solids: Recent Results on Superconducting $YBa_2Cu_3O_x$ Single Crystals

Christoph Meingast

(Received May 15, 2006; Accepted June 17, 2006)

High-resolution thermal expansion measurements of solids provide a very useful and complimentary (to heat capacity) method for studying the thermodynamics of solid-state systems. In this short review, first, different measurement techniques are discussed with special emphasis given to capacitance dilatometry. Then, recent results on the thermal expansion of the high-temperature superconductor (HTSC) $YBa_2Cu_3O_x$ are presented and used to discuss uniaxial pressure effects of T_c, the nature of superconducting fluctuations and oxygen-vacancy ordering in $YBa_2Cu_3O_x$.

1. INTRODUCTION

Thermal expansion is a fundamental thermodynamic property, which is closely tied to the heat capacity. Whereas the heat capacity probes how the entropy responds to temperature changes, thermal expansion probes how the entropy, S, responds to volume changes. This is quantified by the following expression (see *e.g.* Ref.[1])

$$\beta(T) \equiv \frac{1}{V}\left.\frac{\mathrm{d}V}{\mathrm{d}T}\right|_p = \kappa_T \left.\frac{\mathrm{d}S}{\mathrm{d}V}\right|_T \qquad (1)$$

in which $\beta(T)$ is the volume expansivity and κ_T the isothermal compressibility. The entropy in Eq.1 can often be expressed as a sum of the individual entropies of the various subsystems in the solid state (phononic, electronic, magnetic, *etc.*), and there are then contributions to the thermal expansion from each subsystems. Thermal expansion is, thus, very useful for probing the pressure (or volume) dependence of various solid state properties (*e.g.* the Debye frequency, the electronic density of states, the superconducting critical temperature, *etc.*) in the limit of zero applied pressure. For anisotropic systems, thermal expansion data can be used to derive uniaxial pressure effects, which are usually very difficult to measure directly.

One is often confronted with the difficult problem of separating the different contributions from the subsystems in both heat capacity and thermal expansion data. In many cases this is, however, much easier for the thermal expansion than for the heat capacity. For example in HTSC, the electronic contribution to the thermal expansion at T_c is usually significantly larger in comparison to the phononic background than the analogous contribution to the heat capacity. This makes a detailed study of the shape of the superconducting transition, which provides important information about the nature of the superconducting state, much easier using thermal expansion data than heat capacity data.

There are several excellent reviews covering thermal expansion of superconductors.[1-4] The goal here is not to present another comprehensive review, but rather to give the reader a flavor of the kind of results obtainable using high-resolution thermal expansion measurements. For this purpose, new results on HTSC will be discussed.

2. THERMAL EXPANSION MEASUREMENT TECHNIQUES

Thermal expansion can be measured either by monitoring the length changes of a macroscopic sample with a dilatometer or by examining the changes in lattice parameters using X-rays or neutron diffraction. The

best measurement technique depends on the resolution desired and on the type of samples which are available. Typical resolutions vary between $\Delta L/L \approx 10^{-5} \sim 10^{-6}$ for standard diffraction methods and $\Delta L/L \approx 10^{-9} \sim 10^{-10}$ for custom-made capacitance dilatometers. Diffraction methods have the advantage of being able to measure the thermal expansion of a small amount of powder material, from which also the anisotropic thermal expansion can be obtained if the crystal structure is non-cubic. For dilatometry, much larger bulk samples (with minimum dimensions on the order of 1 mm) are needed, and single crystals are required for investigations of the anisotropy in non-cubic systems. For engineering purposes, a resolution of $\Delta L/L \approx 10^{-5} \sim 10^{-6}$ is usually adequate, and either a diffraction method or a standard dilatometer may be used. On the other hand, if one is, for example, interested in observing the superconducting transition in the thermal expansion, one needs to use a device with the highest possible resolution because these effects are usually very small. In the following, I briefly discuss custom-made capacitance dilatometers, which have become the standard device for measuring thermal expansion with very high resolution. For more details concerning this and other techniques, the reader is referred to previous reviews.[1,2,4,5]

Fig.1 shows a schematic diagram of a modern capacitance dilatometer.[6] The basic principle is to mechanically couple the sample to a movable plate of a parallel plate capacitor. As the sample expands or contracts, the gap of the capacitor changes, which can be measured very accurately using a three-terminal capacitance bridge. In contrast to older designs, where the sample formed one plate of the capacitor, this newer design[6,7] allows one to measure samples of arbitrary material, shape and size. Modern bridges can detect a change in capacitance as small as 5×10^{-7} pF, which translates to length change of 5×10^{-12} m for a nominal capacitance of 10 pF at a gap of 100 μm. Thus, if one has a 1 cm long sample, it is in principle possible to measure relative length changes as small as $\Delta L/L \approx 5 \times 10^{-10}$. In practice, however, this theoretical resolution is only achievable under special circumstances. Capacitance dilatometers are usually made out of metal, and the expansion (contraction) of the dilatometer cell must be taken into account. This expansion of the cell can be determined by measuring a known reference material such as Cu, Al or Si, for which very accurate thermal expansion data exists in the literature.[8] The absolute sensitivity of the dilatometer can be determined by measuring two different reference materials (*e.g.* Cu and Si) under identical conditions. To utilize the full length resolution of a capacitance dilatometer, temperature measurement and control must also be optimized. There are two different approaches to temperature control: 1) the temperature is stabilized at a fixed number of points, at which both the length and temperature are recorded

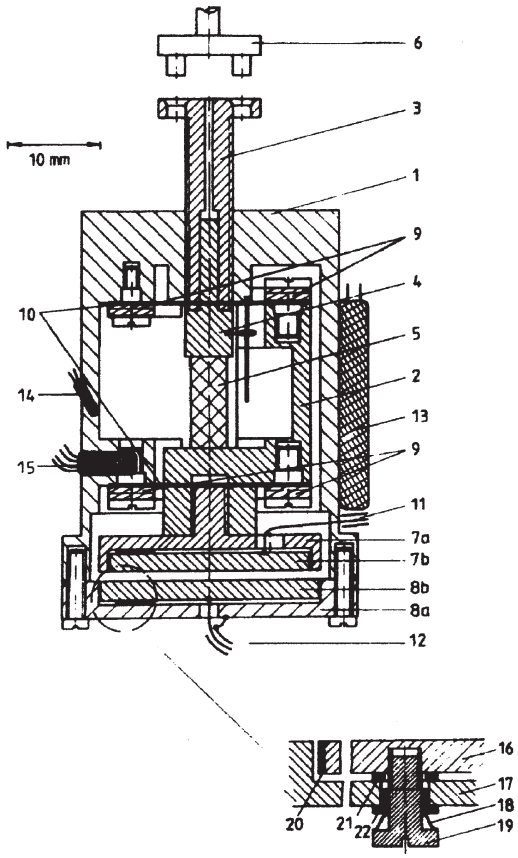

Construction of the cell: 1, frame; 2, movable part; 3, screw; 4, piston; 5, sample; 6, bayonet fitting; 7a, guard ring; 7b, capacitor plate; 8a, guard ring; 8b, capacitor plate; 9, washers; 10, springs; 11,12, electrical leads; 13, platinum resistor; 14, silicon diode; 15, germanium resistor. Inset: 16, capacitor plate; 17, guard ring; 18, spring; 19, screw; 20, Araldite; 21, sapphire spacer; 22, Araldite washer.

Fig.1 Schematic diagram of a modern custom-made capacitance dilatometer. (Adapted from Pott and Schefzyk[6]).

after the system has reached thermal equilibrium, or 2) the temperature is scanned at a fixed rate and both temperature and length change are recorded continuously. The temperature scanning technique has three important advantages: 1) A large number of data points can be obtained in a relative short period of time. This is especially important for studying the details of phase transitions, where the expansivity changes rapidly with temperature (see *e.g.* Ref.[9]). 2) Kinetic effects in the thermal expansion, as *e.g.* found near glass transitions, can easily be studied by varying the heating (cooling) rate of the experiment.[10-12] 3) Temporal capacitance drifts in the cell are less of a problem, since the measurements are made much quicker. The disadvantage of this technique is that the sample and dilatometer are not in thermal equilibrium, which can result in erroneous temperature and length readings. A careful calibration of the dilatometer can, however, eliminate most of these uncertainties. Temperature oscillating techniques, which in principle should be more sensitive due to time averaging and should also eliminate the effects of capacitance drifts, have been utilized in capacitance dilatometry as well.[13] However, the typically very low frequency of such a setup result in extremely long measuring times, and this technique is not widely used presently.

3. THERMAL EXPANSION OF THE HIGH-TEMPERATURE SUPERCONDUCTOR $YBa_2Cu_3O_x$ FROM 5 K TO 500 K: UNIAXIAL PRESSURE EFFECTS, SUPERCONDUCTING FLUCTUATIONS AND OXYGEN ORDERING

The high-temperature cuprate superconductor $YBa_2Cu_3O_x$ is ideally suited for demonstrating the type of results obtainable using capacitance dilatometry, because there are several interesting features in the thermal expansion in $YBa_2Cu_3O_x$ and fairly large high-quality untwinned single crystals are available. $YBa_2Cu_3O_x$ has an orthorhombic crystal structure and, therefore, has three principal linear thermal expansion coefficients (or expansivities), *i.e.* one along each crystallographic axis. The expansivities from 4 K to 500 K of an untwinned $YBa_2Cu_3O_x$ single crystal in fully oxygenated ($x=7.0$; dotted lines) and slightly oxygen deficient ($x=6.95$; solid lines) states are shown in **Fig.2**. The data were obtained with two different temperature-scanning capacitance dilatometers working in the temperature ranges 4 K ~ 300 K and 150 K ~ 500 K, respectively.[9,11] As is apparent from an inspection of **Fig.2**, $\alpha(T)$ is quite anisotropic, being largest along the *c*-axis (perpendicular to the CuO_2 planes) and smallest along the *b*-axis (parallel to the CuO chains). In addition to the regular expansion from the lattice, clear anomalies in $\alpha(T)$ are also observed at the superconducting transitions around 90 K and at a glass-like transition near room temperature, which results from the freezing of oxygen ordering processes in the CuO chain layer.[11] In the following, both of these effects are discussed in more detail.

The anomalies in $\alpha(T)$ at T_c in the *a*-, *b*- and *c*-axes can be used to predict the dependence of T_c upon uniaxial pressure (stress) using the thermodynamic Ehrenfest relationship

$$\frac{dT_c}{dp_i} = \Delta\alpha_i \cdot \frac{V_{mol}T_c}{\Delta C_p} \qquad (i = a,\ b \text{ and } c) \tag{2}$$

where $\Delta\alpha_i$ and ΔC_p are the anomalies in the linear expansivity and constant pressure heat capacity at T_c, respectively, and V_{mol} is the molar volume. Here it is worthwhile to mention that direct uniaxial pressure (stress) experiments, which are quite difficult to perform due to the fragile nature of these crystals, have confirmed the predictions from the expansivity anomalies using the Ehrenfest relation.[14]

So far we have considered the uniaxial pressure (stress) dependencies of T_c, which can be obtained directly from the expansivity anomalies at T_c using Eq.2. To gain further insight into the mechanism behind these pressure (stress) dependencies, it may be very useful to also calculate the uniaxial strain dependencies of T_c, *i.e.* $dT_c/d\varepsilon_i$, where $\varepsilon_i = \Delta l_i / l_i$.[15] In theoretical work, it is usually easier to 'apply' uniaxial strain than uniaxial stress. The difference between the strain and pressure dependencies is that for uniaxial pressure, one applies pressure (stress) in a given direction and allows the other axes to expand naturally via the Poisson effect. For uniaxial strain on the other hand, one axis is compressed while the lengths of the other axes are forced to remain constant. It is straightforward to calculate the strain dependencies from the pressure (stress) dependencies and vice versa using the elastic constants C_{ij}.[15]

$$\frac{dT_c}{d\varepsilon_i} = \sum_{j=1}^{3} C_{ij} \frac{dT_c}{dp_j} \quad (3)$$

It should be noted that the magnitude (but not the sign) of the strain dependencies can be obtained directly from the sound velocity anomalies at T_c.[16,17]

$$\left(\frac{dT_c}{d\varepsilon_i}\right)^2 = -\frac{\Delta v_i}{v_i} \cdot \frac{2C_{ii}T_c}{\Delta C_p} \quad (4)$$

Here, Δv_i is the jump in the longitudinal sound velocity v in the direction i at T_c. The overall consistency of this thermodynamic approach has been nicely demonstrated in the La-Sr-Cu-O system, where thermal expansion, sound velocity, and uniaxial pressure (strain) experiments are available.[18-20] A particularly striking example of the predictive power of the uniaxial pressure effects has also been obtained in the La-Sr-Cu-O system by Locquet *et al.*;[20] the T_c of a thin film of La-Sr-Cu-O was doubled due to the epitaxial strain resulting from the lattice mismatch of film and substrate, in good agreement with the uniaxial pressure dependencies of T_c predicted using thermal expansion data.[18,19] Although these results are impressive, we still do not have a good microscopic understanding of these complex pressure effects in the HTSC;[21] they are nevertheless very useful for testing theoretical models for HTSC.

The low carrier density, the small coherence lengths, the large anisotropy and the high value of T_c make HTSC very susceptible to thermal fluctuations of the order parameter. Thermal expansion has proved to be an ideal tool to study these effects in detail, because the anomalies at T_c in the thermal expansivity (see **Fig.2**) are quite large in comparison to the phonon background expansivity.[9,22] The basic idea is that the expansivity and heat capacity show the same critical scaling near a critical point, *i.e.* close to T_c. This can be understood in terms of the Pippard relation,

$$\frac{C_p}{T_c} = \alpha V_{mol} \frac{dT_c}{dp} + \text{const.} \quad (5)$$

which is the analogue to the Ehrenfest relation for lambda-type transitions.[23] The scaling of C_p and α in Eq.5 really apply only to the electronic contributions; however, since both C_p and α diverge at T_c, Eq.5 in principle also holds for the whole of C_p and α very close to T_c. For $YBa_2Cu_3O_x$ the fluctuation signal-to-background ratio can

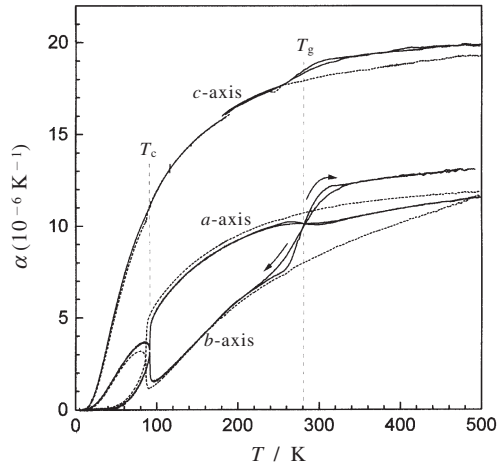

Fig.2 Thermal expansivities along the three crystallographic axes of a untwinned $YBa_2Cu_3O_x$ single crystal between 5 K and 500 K in fully oxygenated ($x = 7.0$; dashed line) and slightly oxygen deficient ($x = 6.95$; solid lines) states. Clear anomalies are seen both at T_c and at a kinetic glass-transition temperature T_g for the oxygen deficient crystal. (Adapted from P. Nagel *et al.*[11])

be further enhanced by considering the difference in expansivities along the *b*- and *a*-axes, and the lambda shape of the transition becomes quite apparent in this quantity $\Delta\alpha_{b-a}$ (see **Fig.3(a)**). Here the signal-to-background ratio is much more favorable than in the heat capacity, where the electronic component is only a few percent of the total heat capacity, and this allows an analysis of the expansivity data without subtracting an unknown phonon background.[9] It is customary to plot the expansivity (or heat capacity) near a critical point versus the logarithm of the absolute value of the reduced temperature $|T-T_c|$, from which it directly seen that one is approximately dealing with a logarithmic divergence of $\Delta\alpha_{b-a}$ at T_c (see **Fig.3(b)**). This is very similar to what is observed in both the heat capacity and expansivity of ^{4}He at the superfluid transition and shows that the superconducting transition in $YBa_2Cu_3O_x$ belongs to the 3D-*XY* universality class, *i.e.* a 3-dimensional system with a two-component (complex) order parameter.[9] Thermal expansion studies also show that these fluctuations become more two-dimensional in the 'underdoped' part of the phase diagram and that they smoothly disappear in overdoped $YBa_2Cu_3O_x$.[22] It is

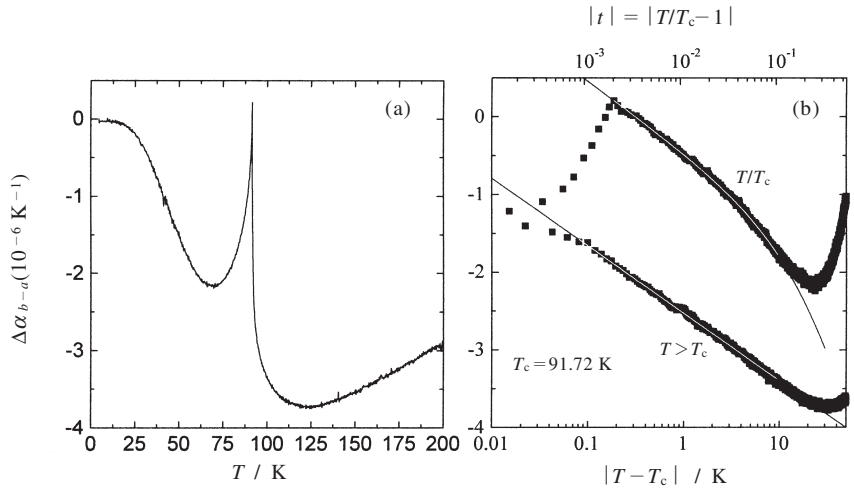

Fig.3 Difference between the thermal expansivities along the *b*- and *a*-axes ($\Delta\alpha_{b-a}$) of an untwinned $YBa_2Cu_3O_{6.95}$ single crystal versus (a) temperature and (b) absolute value of the reduced temperature $|T\text{-}T_c|$. The λ-shape of the anomaly at T_c is an indication for strong thermal fluctuations close to T_c. (Adapted from Pasler *et al.*[9]).

interesting to note that these 3D-*XY* fluctuations are phase fluctuations of the order parameter, which take on the form of topological vortex loops.[24]

It should be mentioned that the pressure dependence of T_c in HTSCs should in principle be extracted using the Pippard relation and not the Ehrenfest relation, since all HTSCs show large fluctuation effects and should, therefore, be classified as λ-transitions. To do this, one usually plots $\alpha(T)$ versus $C_p(T)/T$ near the transition, and dT_c/dp is given directly by the slope in this representation. In practice, however, it makes little difference if one extracts the 'mean-field' jump from the data and uses the Ehrenfest relation or if one uses the whole anomaly and the Pippard relation. Much more important is that both heat capacity and thermal expansion are 1) measured on the same sample and 2) that the anomalies in both $\alpha(T)$ and $C_p(T)$ are treated in a consistent fashion.

Oxygen ordering in the HTSC has received a lot of attention because this ordering strongly affects the carrier density and, thus, superconductivity. Thermal expansion measurements have proved to be ideal for studying both the kinetics and thermodynamics of this ordering processes in $YBa_2Cu_3O_x$, which occur in the CuO chain layer.[11] These processes are responsible for the glass-like transition near room temperature shown in **Fig.2**. From a comparison with the expansivities of the fully oxygenated crystal with $x = 7.0$, which serves as a kind of background since it contains no O-vacancies and thus no vacancy disorder, the contributions from the oxygen-ordering processes between 300 K and 500 K in the $x = 6.95$ crystal become clearly separable from the normal anharmonic phonon expansion. The $\alpha(T)$ contributions from O-ordering ($\alpha_{\text{O-ordering}}(T)$) occur only above T_g, as is typical of glassy behavior. The data show that $\alpha_{\text{O-ordering}}(T)$ is quite anisotropic, and the largest contribution occurs along the CuO chain (*b*-axis) direction. At around 300 K, the kinetics of the ordering becomes comparable to the time scale of the experiment (which was performed in a *T*-scanning mode) and the ordering starts to fall out of equilibrium. Below about 250 K, no ordering occurs on the time scale of the experiment, and, therefore, $\alpha_{\text{O-ordering}}(T)$ disappears at low temperatures. The cooling and heating curves near T_g in **Fig.2** exhibit the typical hysteretic shape seen in glass transitions.[10-12] If one performs the experiment with different cooling (heating) rates, one finds that the inverse of the glass transition temperature $1/T_g$ shifts linearly with the logarithm of the cooling (heating) rates, from which the kinetic parameters (*e.g.* activation energy barrier) of the ordering process can be obtained.[10-12] Further, a detailed analysis of the shape of the expansivity anomaly at a glass transition allows one to obtain all the details of the relaxation kinetics, *i.e.* the degrees of 'non-exponential' and of 'non-linear' relaxation, which are

typical of glassy behavior (see *e.g.* Ref.[12]) in which the thermal expansion at the orientational glass-transition of C_{60} is studied in detail.). This demonstrates the usefulness of *T*-scanning dilatometry also for studying kinetic phenomena.

The large size of $\alpha_{\text{O-ordering}}(T)$ imply a high sensitivity of the ordering process to small volume or lattice parameter changes. The *b*-axis data have the largest anomaly and the data imply that compressing the *b*-axis lattice parameter will increase the degree of order. Due to the small number of O-vacancies involved in the ordering for $x = 6.95$, the entropy involved in the ordering process is quite small, and only a very small effect is expected in the heat capacity,[11] which has not been observed so far. A very large Grüneisen parameter ($\gamma_{\text{O-ordering}} = 17 \sim 43$) is obtained using measured thermal expansion and compressibility data and an estimated heat capacity anomaly.[11] Here the Grüneisen parameter is related to how the typical energy of the ordering process responds to changes in the volume. Newer thermal expansion measurements on $YBa_2Cu_3O_x$ crystals with different oxygen content have been used to map out the oxygen ordering phase diagram.[25]

4. CONCLUSIONS

High-resolution capacitance dilatometry makes it possible to study the thermal expansion of even single crystals in great detail. The seemingly extremely simple quantity $L(T)$ can provide important complimentary (to heat capacity) thermodynamic information about many different solid state properties. For superconductors, thermal expansion has proved very useful for studying uniaxial pressure effects, thermal fluctuations of the superconducting order parameter, oxygen-ordering effects and the complex interplay between structural transitions and superconductivity. Placing a capacitance dilatometer cell into a magnetic field or a high-pressure cell further enhances the utility of high-resolution dilatometry.

ACKNOWLEDGEMENTS

I would like to express my special appreciation to Akira Inaba and other members of the Research Center for Molecular Thermodynamics, Graduate School of Science, Osaka University, for the hospitality during my stay in Osaka. My special thanks go also to S. Tajima and her group for providing the excellent $YBa_2Cu_3O_x$ single crystals over the years, without which this work would not have been possible.

REFERENCES

1) T. H. K. Barron, J. G. Collins, and G. K. White, *Adv. Phys.* **29**, 609 (1980).
2) E. W. Collings, Applied Superconductivity, Metallurgy and Physics of Titanium Alloys: Vol. 1 Fundamentals, Plenum, New York (1986).
3) G. K. White, "Studies of High Temperature Superconductors", Vol.9, Ed. A. Narlikar, Nova, New York, p.121 (1993).
4) G. K. White, "Thermal Expansion in Handbook of Applied Superconductivity", Vol.1, Ed. B. Seeber, Institute of Physics Publishing, Bristol, p.1107 (1998).
5) B. Yates, Thermal Expansion, Plenum (1972).
6) R. Pott and R. Schefzyk, *J. Phys. E: Sci. Instrum.* **16**, 444 (1983).
7) G. Brändli and R. Griessen, *Cryogenics* **13**, 299 (1973).
8) F. R. Kroeger and C. A. Swenson, *J. Appl. Phys.* **48**, 853 (1977); K. G. Lyon, G. L. Salinger, C. A. Swenson, and G. K. White, *J. Appl. Phys.* **48**, 865 (1977).
9) V. Pasler, P. Schweiss, C. Meingast, B. Obst, H. Wühl, A. I. Rykov, and S. Tajima, *Phys. Rev. Lett.* **81**, 1094 (1998).
10) F. Gugenberger, R. Heid, C. Meingast, P. Adelmann, M. Braun, and H. Wühl, *Phys. Rev. Lett.* **69**, 3774 (1992).
11) P. Nagel, V. Pasler, C. Meingast, A. I. Rykov, and S. Tajima, *Phys. Rev. Lett.* **85**, 2376 (2000).
12) C. Meingast, M. Haluska, and H. Kuzmany, *J. Non-Crystall. Solids* **201**, 167 (1996).
13) T. H. Johansen, J. Feder, and T. Jossang, *Rev. Sci. Instrum.* **57**, 1168 (1986).
14) U. Welp, M. Grimsditch, S. Fleshler, W. Nessler, B. Veal, and G. W. Crabtree, *Journal of Superconductivity* **7**, 159 (1994); H. A. Ludwig, R. Quenzel, S. I. Schlachter, F. W. Hornung, K. Grube, W. H. Fietz, and T. Wolf, *J. Low Temp. Phys.* **105**, 1385 (1996).
15) D. P. Seraphim and P. M. Marcus, IBM Journal, p.94 (1962).
16) A. J. Millis and K. M. Rabe, *Phys. Rev. B* **38**, 8908 (1988).
17) L. R. Testardi, *Rev. Mod. Phys.* **47**, 637 (1975).
18) M. Braden, O. Hoffels, W. Schnelle, B. Büchner,

G. Heger, B. Hennion, I. Tankaka, and H. Kojima, *Phys. Rev. B* **47**, 12288 (1993).
19) F. Gugenberger, C. Meingast, G. Roth, K. Grube, V. Breit, T. Weber, and H. Wühl, *Phys. Rev. B* **49**, 13137 (1994).
20) J-P. Locquet, J. Perret, J. Fompeyrine, E. Mächler, J. W. Seo, and G. Van Tendeloo, *Nature* **394**, 453 (1998).
21) See *e.g.* J. Schilling, cond-mat/0604090 (2006) and references therein.
22) C. Meingast, V. Pasler, P. Nagel, A. Rykov, S. Tajima, and P. Olsson, *Phys. Rev. Lett.* **86**, 1606 (2001).
23) A. B. Pippard in "The elements of Classical Thermodynamics", Cambridge University Press (1966).
24) G. A. Williams, *Phys. Rev. Lett.* **82**, 1201 (1999); Z. Tescanovic, *Phys. Rev. B* **59**, 6449 (1999); A. K. Nguyen and A. Sudbø, *Phys. Rev. B* **60**, 15307 (1999).
25) P. Nagel, 2001 Thermodynamics and kinetics of oxygen ordering in $YBa_2Cu_3O_x$ Ph.D thesis, University of Karlsruhe and Forschungzentrum Karlsruhe (also available as a Forschungszentrum Karlsruhe publication - see: www.fzk.de)

Christoph Meingast
Forschungszentrum Karlsruhe, Institut für Festkörperphysik
PO Box 3640, 76021 Karlsruhe
e-mail: meingast@ifp.fzk.de